

## **THERMAL CHARACTERIZATION OF HAIR USING TG-MS COMBINED THERMOANALYTICAL TECHNIQUE**

*Zs. Éhen<sup>1</sup>, Cs. Novák<sup>2\*</sup>, J. Sztatisz<sup>1</sup> and O. Bene<sup>1</sup>*

<sup>1</sup>Institute of General and Analytical Chemistry, Budapest University of Technology and Economics, Szent Gellért tér 4, H-1111 Budapest, Hungary

<sup>2</sup>Hungarian Academy of Sciences, Budapest University of Technology and Economics, Research Group of Technical Analytical Chemistry, Szt. Gellért tér 4, H-1111 Budapest, Hungary

### **Abstract**

Four amino acids and four different hair samples were studied in order to get information about the decomposition of human hair, using combined (TG-MS) and DSC techniques.

The thermal stability of the investigated amino acid samples was different. Since they contain identical functional groups ( $-\text{NH}_2$ ,  $-\text{COOH}$ ) some common mass/charge units were identified. However, due to their different chemical composition remarkable differences have also been obtained.

The results of the investigation of the amino acids were helpful to study the thermal fragmentation of the hair samples. In our experiments, the effect of the heating rates was also studied.

**Keywords:** amino acid, combined techniques, DSC, hair, mass spectrometry, scanning electron microscopy, TG-MS

### **Introduction**

Although the structure of human hair seems to be simple, indeed it's a complex system, an annex of skin. The hair growth rate varies between 0.7 and 3.6 cm/month, in general 1 cm/month is the accepted [1].

As concern to the structure of the hair, it can be divided into two main parts. One is the hair-root and the other is the hair filament. In agreement with our scanning electron microscopic observation (Fig. 1a) the cells covering the outer surface of the hair filament form a tiled-roof-like structure is called cuticle.

The cuticle is a very resistant part of hair against mechanical treatment. Below this thin layer takes place the cortex, which represents the major part of hair and also determines its flexible or tensile strength properties. The internal part of hair is called medulla. The root of the filament is surrounded by the hair onion, which is responsible for keratin producing.

---

\* Author for correspondence: E-mail: cs-novak@mail.bme.hu

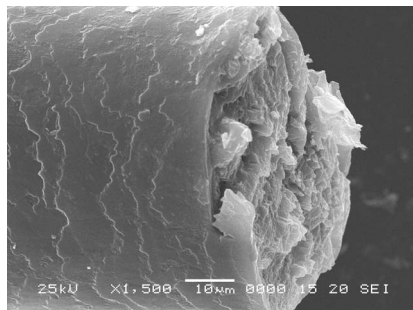


**Fig. 1a** Sample 2 (dyed, black hair)

Although the hair samples differ by their origin (e.g. ethnical, colour, body region) they show many structural similarities. The hair consists of fibrous proteins which are mostly keratins and melanins (eumelanins and pheomelanins) (85–93%), water (3–5%), lipids (1–9%) and mineral compounds (0.25–0.95%) [2].

The morphology of the fibrous structure is demonstrated in Fig. 1b.

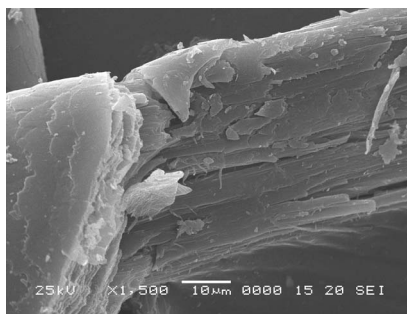


**Fig. 1b** Sample 4 (black hair)

In human hair mainly the following amino acids compose the above mentioned two proteins, melanin and  $\alpha$ -keratin: aspartic acid, cystine, histidine, methionin, glutamic acid and tyrosine. The amino acids form  $\alpha$ -helices, where the internal diameter of the chains is approximately 0.54 nm. This space is sufficiently enough to entrap guest molecules as medicines or their metabolites [3, 4]. This structural arrangement allows detecting drugs or their metabolites from hair samples.

The importance of the hair analysis originates from a serious social problem, namely the long term time control of drug addicts. For this control originally the analysis of liquid-state (blood, urine and sweat) samples was developed using HPLC/HPLC-MS and GC/GC-MS methods, which give information of a 3–7 days long period after the last drug abuse [5–7].

Since medicine and drug metabolites from blood-stream get and infiltrate into the hair, depending on the length of the hair it makes possible to collect information from a longer period in contrast to urine or blood analysis.

The analysis of hair samples requires transforming them from solid- to liquid-state, which can be revealed using acidic, alkaline or enzymatic digestion.

Over all above mentioned, the complicated matrices and the different cultural, hygienic habits, furthermore the frequency of drug taking influence the infiltration of metabolism products making the evaluation even more difficult [6].

The application of TG-MS combined technique provides the advantage of avoiding the multistage sample preparation. Instead of the application of different digestion methods, an appropriate amount of solid hair is required, which has to be cut into small pieces and simply put into the sample holder.

In the recent literature very few papers deal with the thermal analysis of human hair. Some results are written by Cao [4] and Wright *et al.* [8] using DSC, TG methods. Thermal behaviour of sheep wool was reported by Tonin *et al.* [9]. (Obviously, the origin of the sheep wool is different. However, due to its similar morphology and high melanin/keratin content, among natural substances the sheep wool is the closest to the human hair with regards to its general properties and structure.)

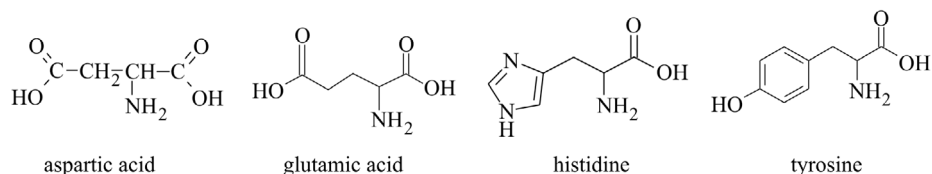
In the present study we aimed to carry out a preliminary study concerning the applicability of combined thermoanalytical techniques in the investigation of different hair samples.

## Experimental

### Materials

In the present study four amino acids (analytical grade) and four hair samples were investigated.

The structure of the measured amino acid components:



**Scheme 1** Chemical structure of the investigated amino acids

The origin of the different hair samples:

- Sample 1 – blond hair, 18 years old woman
- Sample 2 – black, dyed hair, 40 years old woman
- Sample 3 – brown hair, 35 years old man
- Sample 4 – black, 10 years old child

The samples were collected from posterior vertex region of scalp, cut as close as possible to the skin and stored at room temperature.

### *Instruments*

The thermoanalytical measurements have been carried out using TA Instruments (Newcastle, Delaware, USA) DSC 2920 cell and STD 2960 simultaneous TG-DTA unit using helium purging (flow rate: 10 L h<sup>-1</sup>). For the evolved gas analysis measurements the STD 2960 unit was connected to a Balzers Thermostar GSD 300T quadrupole mass spectrometer. The evolved gases from the simultaneous module were transferred to the mass spectrometer through a heated silica capillary inlet.

The mass spectrometer has been operated in two different modes.

In 'scan analogue' mode the ion current in selected specific mass/charge range was continuously measured and described as a function of  $m/e$  starting from a previously given  $m/e$  value along a selected mass range.

When multiple ion detection (MID) mode was used, the ion current belonging to the previously selected individual  $m/e$  channels were detected and described as a function of time.

The data collection for the MS measurements has been done as function of time, which is proportional to the temperature of the sample. So far the SAC and MID curves can be easily compared to TG/DTG runs.

The scanning electron microscopic observations have been performed on a Jeol JSM 5500LV apparatus after sputtering of Au/Pd on the investigated samples.

The experimental conditions are collected in Table 1.

For SAC and MID measurements the observation time was 0.2 sec for each channel.

**Table 1** Experimental parameters

	Amino acid samples	Hair samples	
Heating rate/K min <sup>-1</sup>	5	5	50
Temperature interval/°C	35–350	35–350	35–400
Sample mass/mg	5–8	5–10	
Observed specific mass range/amu	10–140	10–100	

## **Results**

### *Investigation of amino acids*

#### Thermoanalytical results

In order to get more information about the thermal behaviour of hair samples it was decided to examine some of the previously mentioned amino acids.

The representative thermoanalytical curves are given in Fig. 2.

It can be seen that except tyrosine all analysed amino acids show well separated decomposition steps. The mass losses in the observed temperature range were quite

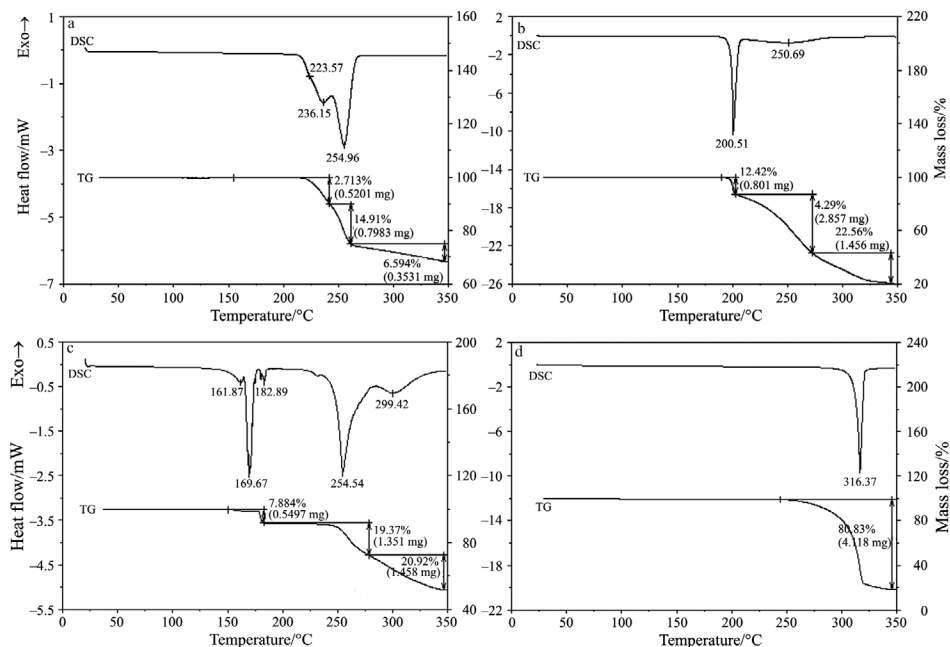


**Fig. 2** Thermal behaviour of amino acid samples; a – aspartic acid, b – glutamic acid, c – histidine, d – tyrosine

different. While the least mass loss was observed for aspartic acid (31%), whilst the highest mass loss was measured for glutamic acid (78.3%).

Consequently, the DSC peaks appeared in a wider temperature range showing the endothermic decomposition of the substances. Glutamic acid and the aromatic tyrosine show one edgy peak, but in the previous case the sharp endotherm is followed by a diffuse endotherm effect. One can notice that both aspartic acid and histidine possess overlapping peaks. By the comparison of the thermoanalytical curves it was concluded that histidine has the least thermal stability, since its decomposition starts at about 150°C. The highest thermal stability was observed for tyrosine, since no mass loss was obtained up to 230°C.

#### Mass spectrometric results

The mass spectrometric behaviour of the investigated amino acids (Fig. 3) showed significant differences compared to [10]. The main reason for the observed differences is caused by the currently used experimental arrangement, since in our case the products of the primary or secondary decomposition reach the detector of the mass spectrometer.

Alas the chemical structure of the measured amino acids were different, all of them contain amino and carboxyl groups. So far, it can be expected that by the evaluation of their mass spectra some common  $m/e$  signals appear, which is representative to the presence of the amino and carboxylic groups. At the same time signals appear

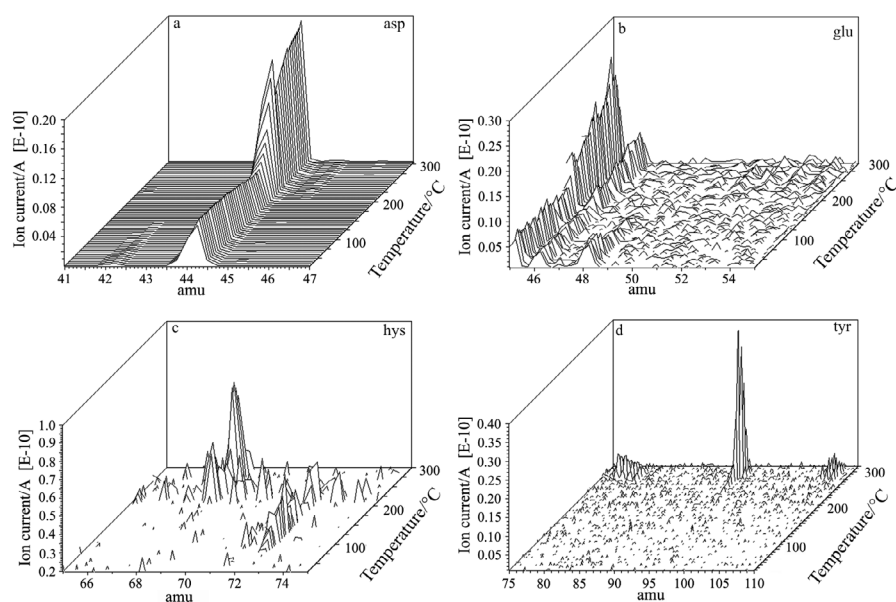


**Fig. 3** 3D scan spectra of amino acid samples; a – aspartic acid, b – glutamic acid, c – histidine, d – tyrosine

at different  $m/e$  values due to their different chemical composition. Similar and specific signals are collected in Table 2.

A possible interpretation of  $m/e$  values collected in Table 2 is given in Table 3.

**Table 2** Possible fragmentation of amino acids

$m/e$	16	17	18	44	45	46	68–69	72	77–80	94	106–108
Aspartic acid	+	+	+	+	+	+					
Glutamic acid	+	+	+	+	+	+					
Histidine	+	+	+	+	+	+	+	+			
Tyrosine	+	+	+	+	+	+			+	+	+

### *Investigation of hair*

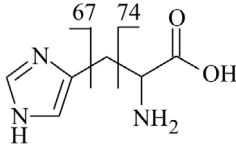
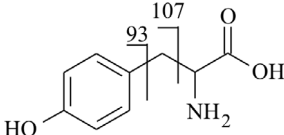
#### Thermoanalytical results

The TG and DSC curves of the hair samples are collected in Fig. 4. It can be seen that their shape are very similar.

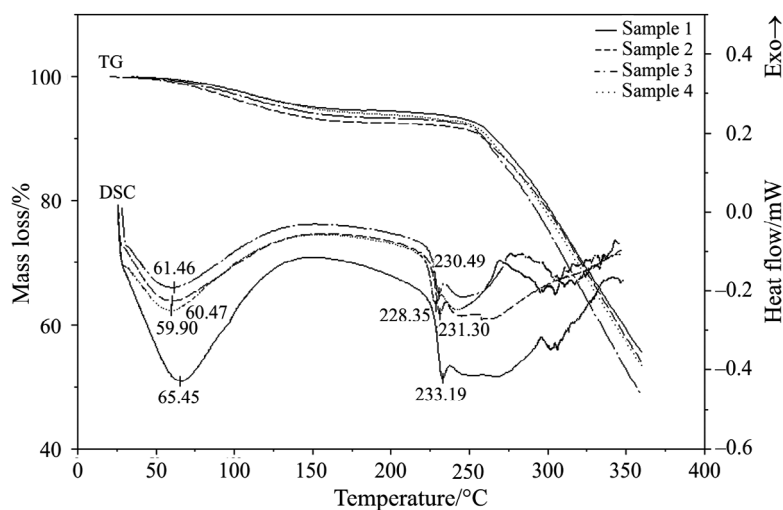
Between 30 and 120°C 5–8% mass losses were recorded causing endotherm effects on the DSC curves, assigned to the evolution of the absorbed water content of the hair.

The first local endotherms between 230–233°C, in the broad endothermic region can be attributed to the melting of  $\alpha$ -keratin. On further heating the thermal de-

**Table 3** A possible interpretation of  $m/e$  values collected in Table 2

$[-\text{NH}_2]^+$	$m/e=16$
$\text{OH}_2^+$	$m/e=18$
$\text{HO}-\text{C}\equiv\text{O}^+$	$m/e=45$
$\text{O}-\text{C}\equiv\text{O}^+$	$m/e=44$
	$m/e=67; 74$
	$m/e=93; 107$

composition of the hair started over 250°C. The process was not completed up to 350°C. At this temperature 45–55% total mass losses were recorded. In the range of 220–350°C the shape of the curves is characteristic for the thermoanalytical behaviour of the hair samples. At the end of the heating cycle the lookout of the residue

**Fig. 4** TG and DSC curves of hair samples

remained very similar to the initial samples. In the dark-brown residues melted portions could not be differentiated.

In agreement with the thermal results the mass spectra confirm the similar fragmentation behaviour of the hair samples. In order to illustrate the similar mass spectrometric behaviour of the hairs, representative parts of the scan analogue records (SAC) of Sample 1 and Sample 2 are given in Fig. 5.

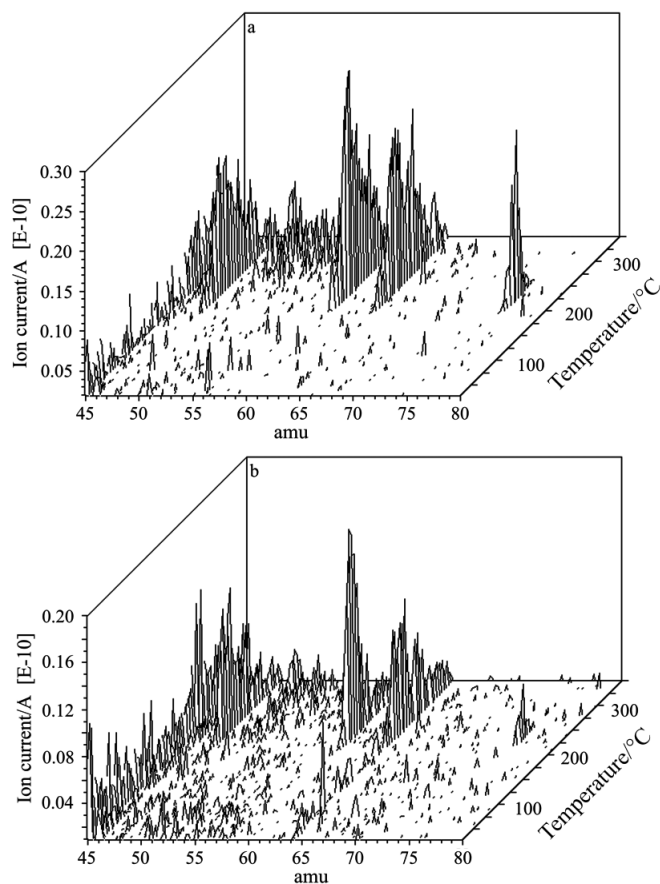


**Fig. 5** Scan analogue spectra of a – Sample 1 and b – Sample 2 ( $\beta=5^{\circ}\text{C min}^{-1}$ )

By the evaluation of the mass spectra it can be stated that the most representative signals appeared at  $m/e=34, 48, 60, 64$  and  $76$ . Furthermore the highest ion current values were measured for these units. These peaks can also be observed on the conventional mass spectrum of  $\alpha$ -keratin [11]. For the assignment of these peaks the mass spectra of the pure amino acid samples were used. As it has been mentioned above  $m/e=34, 48, 64, 76$  units are characteristic for cystein, a sulphur containing amino acid [10], whereas  $m/e=60$  unit may possibly representative for histidine (Fig. 3c).



According to the mass spectra in the specific mass range of 10–100 the 34, 48, 64 and 76  $m/e$  values are characteristic for hair. A possible interpretation of the proper peaks can be seen in representing the main amino acid components in the structure as it can be seen in Fig. 6.

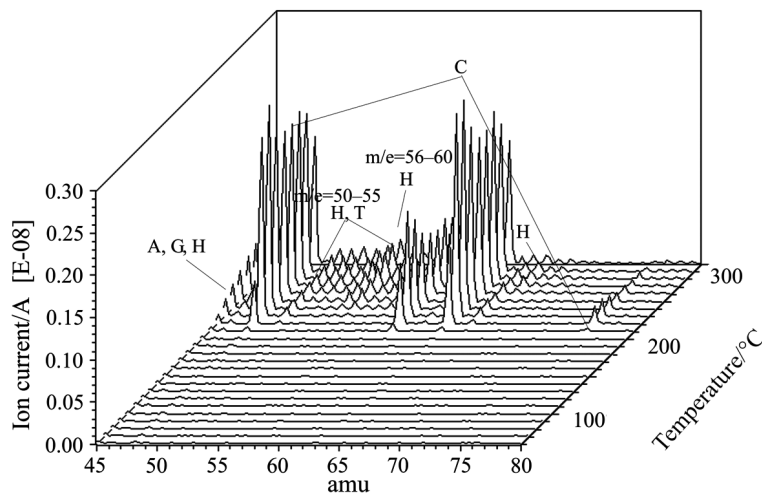


**Fig. 6** Hair sample 1,  $\beta=50^{\circ}\text{C min}^{-1}$ , interpretation of specific mass units; (A – aspartic acid, G – glutamic acid, H – histidine, T – tyrosine)

Besides identifying the fragments the effect of the heating rate on the fragmentation behaviour of the samples was also investigated. Experiments have been carried out using 5 and 50  $\text{K min}^{-1}$  heating rates.

The corresponding TG and DTA curves are summarized in Fig. 7. Applying higher heating rate the decomposition of the investigated samples is shifted towards higher temperatures by  $30^{\circ}\text{C}$ . In agreement with the literature data [11] the melting peak of the  $\alpha$ -keratin appeared at  $233^{\circ}\text{C}$  when the lower heating rate was used and shifted up to  $250^{\circ}\text{C}$  when  $50 \text{ K min}^{-1}$  heating rate was applied.

The total mass losses measured at  $350^{\circ}\text{C}$  were also influenced by the different heating rates. The corresponding DTA peak temperatures and mass loss values are collected in Table 4. These latter ones indicate that higher mass losses were obtained when  $5 \text{ K min}^{-1}$  heating rate was applied.

Due to the higher heating the time of measurement decreased, but the corresponding ion currents remarkably increased. The ion current values normalized to 1 mg sample mass are summarized in Table 5.

Figures 8 and 9 indicate the effect of different heating rates. It can be seen that applying  $50 \text{ K min}^{-1}$  heating rate the measured ion currents are higher with about two orders of magnitude. The higher heating rate resulted higher concentration of fragments in the vapour phase inside the furnace. Consequently larger amount of sample was transferred to the mass spectrometer during a unit of time.

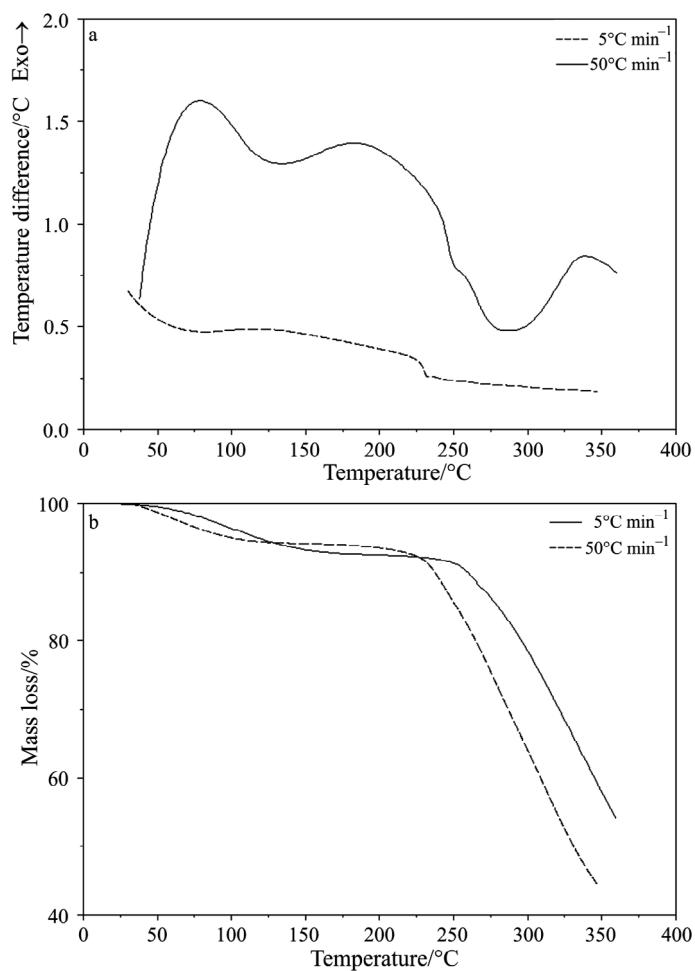


Fig. 7 a – DTA and b – TG curves of Sample 1 at different heating rates

Table 4 Mass loss values measured at 350°C using different heating rates

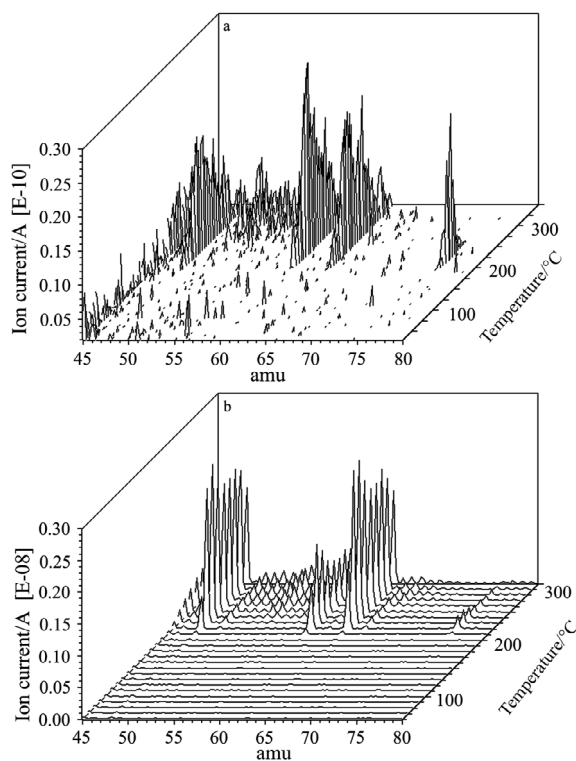
Heating rate/°C min <sup>-1</sup>	Sample	DTA		Mass loss/%	
		Endothermic peak/°C		1. step	2. step
5	1.	83.7	233.2	5.3	49.0
	2.	79.6	231.3	5.3	49.6
	3.	80.8	230.1	7.1	53.5
	4.	77.2	228.9	5.7	50.8
50	1.	134.9	250.4	5.1	35.6
	2.	117.6	250.8	7.1	34.7
	3.	132.9	250.1	5.8	36.9
	4.	139.7	247.4	6.5	40.9

**Table 5** Normalized ion currents for Sample 1 and 2

Heating rate/K min <sup>-1</sup>	Sample	Intensity of ion current/A			
		<i>m/e</i> =48	<i>m/e</i> =60	<i>m/e</i> =64	<i>m/e</i> =76
5	1.	1.97E-12	7.87E-12	2.36E-12	2.36E-12
50	1.	4.01E-10	2.17E-10	4.17E-10	4.51E-11
5	2.	1.32E-12	1.93E-12	1.22E-12	5.89E-13
50	2.	8.59E-10	6.79E-10	8.97E-10	1.79E-10

Nevertheless the heating rate has another effect, since it changed the relative intensities of the peaks. The difference is not significant comparing the ratio of  $I_{48}:I_{64}$ , but remarkable for  $I_{48}:I_{60}$  and  $I_{60}:I_{64}$ . The corresponding ion currents are summarized in Table 6.

The effect of heating rate can be followed also in the MID curves (Figs 10, 11). Therefore discrepancy can be seen considering the shape of an ion current curve related to a characteristic mass unit at the same sample by applying different heating rates.

**Fig. 8** Scan analogue spectra of Sample 1 a –  $\beta=5$  K min<sup>-1</sup>, b –  $\beta=50$  K min<sup>-1</sup>

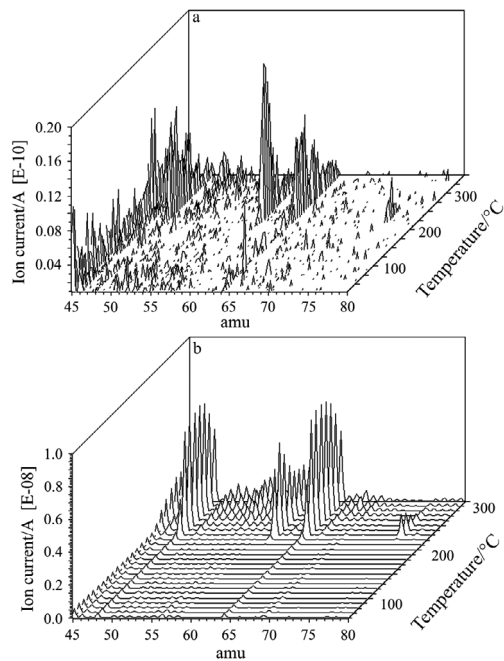


**Fig. 9** Scan analogue spectra of Sample 2 a –  $\beta=5 \text{ K min}^{-1}$ , b –  $\beta=50 \text{ K min}^{-1}$

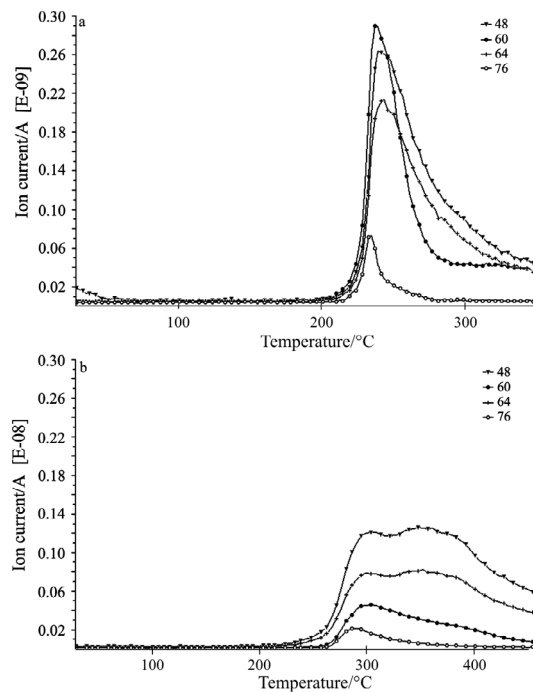


**Fig. 10** MID spectra of Sample 1 a –  $\beta=5 \text{ K min}^{-1}$ , b –  $\beta=50 \text{ K min}^{-1}$

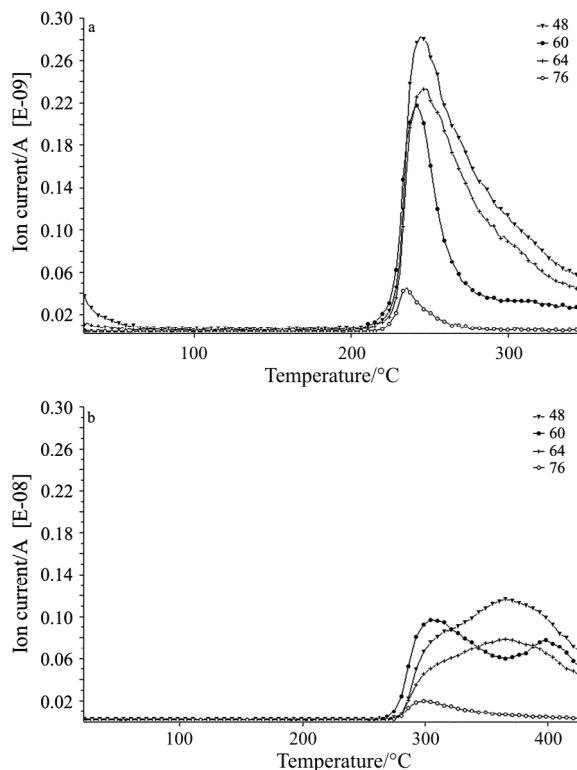


Fig. 11 MID spectra of Sample 2 a –  $\beta=5 \text{ K min}^{-1}$ , b –  $\beta=50 \text{ K min}^{-1}$

One more observation, which can be attributed not only for the different heating rates that the shape and arrangement of the MID curves of Samples 1 and 2 are practically the same, while it was changed when  $50 \text{ K min}^{-1}$  heating rate was applied.

These differences can be explained by the different origin and treatment (Sample 2 was a dyed hair) of the hair samples.

Table 6 Ion current ratios for different amu-s

Heating rate/ $^{\circ}\text{C min}^{-1}$	48:60 ratio	60:64 ratio
5	1:4	3:1
50	2:1	1:2

## Conclusions

Analyzing the DSC and TG curves of amino acids, it can be seen that all substances possess an endothermic decomposition accompanied by different losses. Among the investigated amino acids histidine showed the least and tyrosine the highest thermal

stability. Interpreting the mass spectra of the amino acids, their most representative specific mass/charge units could be selected.

The thermoanalytical curves of different hair samples showed no substantial differences in their thermal behaviour. Smaller differences were found in their moisture content and the temperatures of endothermic peaks belonging to the melting of  $\alpha$ -keratin.

Comparing the mass spectra of  $\alpha$ -keratin and the hair samples the most representative signals appeared at the same  $m/e$  units. Based on the mass spectra of the investigated amino acids some representative signals on the mass spectra of the hair samples could be identified.

Concerning the effect of the different heating rates, it can be stated that the higher heating rate caused:

- two orders of magnitude higher ion current
- change in the relative intensities of some peaks
- alteration in the curvature of the MID lines.

The observed differences can be attributed to the different origin of samples. These preliminary results can be a possible starting point in the analysis of the infiltrated medicines and their metabolites in hair. However, in this case, the geographic and ethnic origin, moreover the effect of treatment using different substances (e.g. dying) should be taken into account.

\* \* \*

The authors are thankful to Katalin Marthi for her constructive help in SEM.

## References

- 1 H. Schütz, B. Ahrens, F. Erdmann and G. Rochholz, *Pharmazie Z.*, 22 (1993) 65.
- 2 R. Wennig, *Forensic Sci. Int.*, 107 (2000) 5.
- 3 F. P. Smith and R. H. Liu, *J. Forensic Sci.*, 31 (1986) 1269.
- 4 J. Cao, *Thermochim. Acta*, 335 (1999) 5.
- 5 P. Kintz, *Ther. Drug Monit.*, 18 (1996) 450.
- 6 Y. Takiguchi, R. Ishihara, R. Kato, S. Kamihara, M. Yokota and T. Uematsu, *J. Pharm. Sci.*, 90 (2001) 1891.
- 7 Y. Nakahara, *J. Chromatogr. B*, 733 (1999) 161.
- 8 S. F. Wright, K. A. Alexander and D. Dollimore, *Thermochim. Acta*, 367–368 (2001) 29.
- 9 C. Tonin, A. Aluigi, M. Bianchetto Songia, C. D'Arrigo, M. Mormino and C. Vineis, *J. Therm. Anal. Cal.*, 77 (2004) 987.
- 10 Mass Spectral Browser version 3.1d, The Wiley Registry of Mass Spectral Data 6<sup>th</sup> Edition with Structures.
- 11 H. L. C. Meuzelaar, J. Haverkamp and F. D. Hileman, *Pyrolysis Mass Spectrometry of Recent and Fossil Biomaterials*, Elsevier, 1982, p. 164.